Communications on Applied Nonlinear Analysis
ISSN: 1074-133X
Vol 32 No. 1s (2025)

Exploring the Complex Dynamics of Julia and Mandelbrot Sets for the Complex-valued Mapping $\sin(z^k) + az + c$ Using Four-Step Iterative Scheme with s-Convexity

Nabaraj Adhikari *

Central Department of Mathematics, Institute of Science and Technology

Tirbhuvan University, Kathmandu, Nepal

E-mail: nabaraj.adhikari@cdmath.tu.edu.np (N. Adhikari)

Received: 07-08-2024, Revised: 25-09-2024, Accepted: 10-10-2024

Abstract

In this paper, we investigate unique variations of the Julia and Mandelbrot sets, establishing criteria for the escape of a function $T_c z = \sin(z^k) + az + c$ for all $z \in \mathbb{C}$, where $k \in \mathbb{N} \setminus \{1\}$ and $a, c \in \mathbb{C}$ with $a \neq 0$ by utilizing a four-step iterative scheme extended with s-convexity, we analyze the dynamics of these fractals by formulating and implementing the algorithms. Our exploration focuses on understanding how distinct parameters impact these fractals' color, dynamics, and overall visual characteristics. Our findings reveal that specific fractal patterns resemble exquisite natural objects like flowers and spiders. These fractal designs are also employed as visually striking artistic motifs on garments and textile materials. The captivating and complex properties of fractal patterns within dynamic systems make them an enticing and visually appealing area of research.

Keywords: Julia set; Mandelbrot set; Four-step iteration scheme with s-convexity
.
Mathematics Subject Classification: 28A80; 37F10; 47H10;.

1 Introduction

Fractals have developed as one of the most exciting fields of study because of its self-similarity. In 1917, Julia [6] and Fatou [5] began researching complex-valued maps.

*Corresponding author *E-mail*: nabaraj.adhikari@camath.tu.edu.np

They focused on exploring the complex dynamics of complex-valued map, specifically the iterative approximations of the function $z^2 + c$, where z is complex variable and c is a complex constant; however, he faced challenges when attempting to visually present it due to the lack of computer. After Julia's initial exploration, the field of complex dynamics experienced a period of decreased activity lasting for five decades. However, in the 1980s, complex dynamics experienced a revival, spearheaded by Mandelbrot [11], re-emerging as a lively area of mathematical research. This resurgence persists today, driven in part by advancements in computer technology that provide substantial computational power, allowing for the revelation of the intricate beauty of complex dynamics for the first time. He named these complex structure as "fractals" and discovered that the Julia sets have individually in their features for different values of the parameter c. Furthermore, by interchanging the role of z and c, a new set obtained using same iterative scheme, which is called the Mandelbrot set. In 1987s, Lakhtakia *et al.*[9] extended the work of Julia and Mandelbrot for the complex valued function $z^k + c$ for all $z \in \mathbb{C}$, $k \in \mathbb{N} \setminus \{1\}$ and c is complex parameter. Many academics have studied the Julia and Mandelbrot set in depth from different angles ever since it was first introduced. In 2004, Rani and Kumar [14], began an approach that included using iteration algorithms based on fixed-point theory. This strategy was one of the avenues explored in the analysis of the Julia and Mandelbrot set. After that, different iterative methods are used to create different sorts of fractals, like as Ishikawa-iteration [13], Noor-iteration [4], Abbas iteration[7]. Many researcher use various iterative methods such as Picard-Mann iteration [21], the Picard-Mann iteration with s-convexity [15], and the Picard-Ishikawa iteration [1], viscosity approximation method [8], Jungck-Noor iteration with s-convexity [18], Jungck-CR [17], have all been used to generate the Julia and Mandelbrot sets. Tomar *et al.* [19] flourished escape criteria for the complex-valued function $\sin(z^k) - az + c$, for all $k \in \mathbb{N} \setminus \{1\}$ using Noor-iteration, created and examined numerous Mandelbrot sets. In order to estimate a fixed point for a contraction mapping with a weak type, Shatanawi *et al.*[16] have been introduced a four-step iterative technique. By incorporating s-convexity into a four-step iterative technique, Tomar *et al.* [20] proved an escape criterion for complex-valued cosine function and generate fascinating fractal formations, including Julia and Mandelbrot sets. Recently Adhikari and Sintunavarat create and analyze the properties of fractal for modified functions (see details in [3] [2]).

The paper employs a systematic approach, integrating the four-step iterative method with s-convexity, to investigate novel variations of the Julia and Mandelbrot sets. The primary objective is to define criteria for determining escape conditions for the function $\sin(z^k) + az + c$ for all $z \in \mathbb{C}$ and k is a natural number excluding 1, and a, c are complex constants with $a \neq 0$. The study aims to devise and execute algorithms capable of generating these fractal patterns, thereby expanding the scope for analyzing these captivating fractal structures.

The paper is structured into several sections. Section 2 offers an overview of the notation and definitions employed throughout the article. Section 3 introduces the definition and proves the escape criterion and algorithm used for fractal generation.

Section 4 provides visual examples that illustrate the behavior and patterns produced by the proposed methodology. Finally, Section 5 summarizes the main results and contributions of the research.

2 Preliminaries

In this paper, $\mathbb{C}$, $\mathbb{R}, \mathbb{N}$, always stand for the set of complex numbers, all real numbers, all positive integers, respectively. In this section, we define Julia set, Mandelbrot set, s- convexity and four-step iteration which is use in this research paper.

Definition 2.1 ([6]). The set of complex numbers in which the orbit of function $T_c : \mathbb{C} \to \mathbb{C}$, where $c \in \mathbb{C}$ not diverges towards infinity is referred to as the filled Julia set of T_c. It is denoted by $\mathbb{J}_{T_c}$ and write

$$\mathbb{J}_{T_c} = \{z \in \mathbb{C} : \{|T_c^n(z)|\}_{n=0}^{\infty} \text{ is bounded}\}.$$

Definition 2.2 ([11]). Let $T_c : \mathbb{C} \to \mathbb{C}$ be a complex mapping ,where $c \in \mathbb{C}$ is a parameter. The Mandelbrot set is defined as

$$\mathbb{M} = \{c \in \mathbb{C} : \mathbb{J}_{T_c} \text{ is connected}\}.$$

Equivalently, the Mandelbrot set $\mathbb{M}$ can be defined in [10] as:

$$\mathbb{M} = \{c \in \mathbb{C} : T^n(\kappa) \nrightarrow \infty \text{ as } n \to \infty\}$$

where, κ is any critical point of T_c.

In the year 2020, the following four-step iterative approach was proposed by Shatanawi *et al.* [16] for the approximating a fixed point within a weak-type contraction mapping.

Definition 2.3 ([16]). Let $T_c : \mathbb{C} \to \mathbb{C}$ to be a complex-valued self-mapping. For initial point $z_0 \in \mathbb{C}$ The four-step iteration scheme for sequence $\{z_n\}$ with constant parameter is defined as:

$$\begin{cases} u_n = (1-\delta)z_n + \delta T_c z_n \\ v_n = (1-\gamma)z_n + \gamma T_c u_n \\ w_n = (1-\beta)z_n + \beta T_c v_n \\ z_{n+1} = (1-\alpha)z_n + \alpha T_c w_n \end{cases} \tag{2.1}$$

for all $n \in \mathbb{N} \cup \{0\}$ and $\alpha, \beta, \gamma, \delta \in (0, 1]$.

Definition 2.4 ([12]). Let $z_1, z_2, z_3, \cdots, z_n \in \mathbb{C}$ and $s \in (0, 1]$. The s-convex combination is defined by

$$\lambda_1^s \cdot z_1 + \lambda_2^s \cdot z_2 + \lambda_3^s \cdot z_3 + \cdots + \lambda_n^s \cdot z_n \tag{2.2}$$

where, $\lambda_k \geq 0$ and $\sum_{k=1}^{n} \lambda_k = 1$. When $s = 1$, the s-convex combination reduced to the standard combination.

Recently, Tomar *et al.* [20] added the s-convex combination to the four-step iteration, which is defined as follows:

Definition 2.5 ([20]). $T_c : \mathbb{C} \to \mathbb{C}$ to be a complex-valued self-mapping. For initial point $z_0 \in \mathbb{C}$, the four-step iteration scheme with s-convexity for sequence $\{z_n\}_{n=0}^{\infty}$ with constant parameter is defined as:

$$\begin{cases} u_n = (1-\delta)^s z_n + \delta^s T_c z_n \\ v_n = (1-\gamma)^s z_n + \gamma^s T_c u_n \\ w_n = (1-\beta)^s z_n + \beta^s T_c v_n \\ z_{n+1} = (1-\alpha)^s z_n + \alpha^s T_c w_n \end{cases} \tag{2.3}$$

for all $n \in \mathbb{N} \cup \{0\}$ and $\alpha, \beta, \gamma, \delta, s \in (0, 1]$.

Using the iterative scheme (2.3) they prove the escape criterion for the complex-valued cosine function $\cos(z^k) + az + c$ for all $z \in \mathbb{C}$, $k \in \mathbb{N} \setminus \{1\}$ and $a, c \in \mathbb{C}$ and create the Julia sets, along with Mandelbrot sets.

If $u, v, w, z \in \mathbb{C}$ then by Taylor series expansion for the sine function, we have

$$\begin{aligned} |\sin(u^k)| &= \left| u^k - \frac{u^{3k}}{3!} + \frac{u^{5k}}{5!} - \cdots \right| \\ &= |u^k| \left| 1 - \frac{u^{2k}}{3!} + \frac{u^{4k}}{5!} - \cdots \right| \\ |\sin(v^k)| &= |v^k| \left| 1 - \frac{v^{2k}}{3!} + \frac{v^{4k}}{5!} - \cdots \right| \\ |\sin(w^k)| &= |w^k| \left| 1 - \frac{w^{2k}}{3!} + \frac{w^{4k}}{5!} - \cdots \right| \\ |\sin(z^k)| &= |z^k| \left| 1 - \frac{z^{2k}}{3!} + \frac{z^{4k}}{5!} - \cdots \right| \end{aligned}$$

Suppose

(i) $\left| 1 - \frac{u^{2k}}{3!} + \frac{u^{4k}}{5!} - \cdots \right| \geq |\omega_1|$

(ii) $\left| 1 - \frac{v^{2k}}{3!} + \frac{v^{4k}}{5!} - \cdots \right| \geq |\omega_2|$

(iii) $\left| 1 - \frac{w^{2k}}{3!} + \frac{w^{4k}}{5!} - \cdots \right| \geq |\omega_3|$

(iv) $\left| 1 - \frac{z^{2k}}{3!} + \frac{z^{4k}}{5!} - \cdots \right| \geq |\omega_4|$

where, $|\omega_1|, |\omega_2|, |\omega_3|, |\omega_4| \in (0, 1]$.

3 Main Results

In this section, we prove the escaping criteria, which plays a vital role in creating the Julia and Mandelbrot sets.

3.1 Escape Criteria for Complex Sine Functions

Theorem 3.1. *Let $T_c : \mathbb{C} \to \mathbb{C}$ be a complex-valued map defined by $T_c(z) = \sin(z^k) + az + c$ for all $z \in \mathbb{C}$, $k \in \mathbb{N} \setminus \{1\}$ and $a, c \in \mathbb{C}$ such that $a \neq 0$. Consider the iterative sequence defined in (2.3) and $|\omega_1|, |\omega_2|, |\omega_3|, |\omega_4| \in (0, 1]$ If*

$$|z_0| > \max\left\{|c|, \left(\frac{2(1+|a|)}{s\alpha|\omega_1|}\right)^{\frac{1}{k-1}}, \left(\frac{2(1+|a|)}{s\beta|\omega_2|}\right)^{\frac{1}{k-1}}, \left(\frac{2(1+|a|)}{s\gamma|\omega_3|}\right)^{\frac{1}{k-1}}, \left(\frac{2(1+|a|)}{s\delta|\omega_4|}\right)^{\frac{1}{k-1}}\right\}$$

then $\lim_{n\to\infty} |z_n| = \infty$.

Proof. For $n = 0$ in (2.3) and using the binomial expansion for any index, we obtain

$$\begin{aligned}
|u_0| &= |(1-\delta)^s z_0 + \delta^s T_c z_0| \\
&= |(1-\delta)^s z_0 + \delta^s(\sin(z_0^k) + az_0 + c)| \\
&\geq \delta^s |\sin z_0^k + az_0 + c| - (1-\delta)^s |z_0| \\
&\geq \delta^s |\sin(z_0^k) + az_0 + c| - (1 - s\delta)|z_0| \quad [\because (1-\delta)^s \leq 1 - \delta s] \\
&\geq \delta^s[|\sin(z_0^k)| - |a||z_0| - |c|] - |z_0| + s\delta|z_0| \\
&\geq s\delta[|\sin(z_0^k)| - |a||z_0| - |z_0|] - |z_0| + s\delta|z_0| \\
&= s\delta|\sin(z_0^k)| - s\delta|a||z_0| - s\delta|z_0| - |z_0| + s\delta|z_0| \\
&\geq s\delta|\sin(z_0^k)| - |a||z_0| - |z_0|. \qquad (3.1)
\end{aligned}$$

We have $|\sin(z_0^k)| = |z_0^k|\left|1 - \frac{z_0^{2k}}{3!} + \frac{z_0^{4k}}{5!} - \cdots\right| \geq |z_0^k||\omega_4|$, where $|\omega_4| \in (0, 1]$ except the value for which $|\omega_4| = 0$ and $|z_0| > \left(\frac{2(1+|a|)}{s\delta|\omega_4|}\right)^{\frac{1}{k-1}}$, from inequality 3.1 we obtain

$$\begin{aligned}
|u_0| \geq& s\delta|\omega_4||z_0^k| - (1+|a|)|z_0| \\
=& |z_0|[s\delta|\omega_4||z_0^{k-1}| - (1+|a|)] \\
\geq& |z_0|[2(1+|a|) - (1+|a|)] \\
=& (1+|a|)|z_0| \\
\geq& |z_0|. \qquad (3.2)
\end{aligned}$$

Moving forward to the subsequent stage of the four-step iteration, we have

$$\begin{aligned}
|v_0| &= |(1-\gamma)^s z_0 + \gamma^s T_c u_0| \\
&= |(1-\gamma)^s z_0 + \gamma^s(\sin(u_0^k) + au_0 + c)| \\
&\geq \gamma^s |\sin(u_0^k) + au_0 + c| - (1-\gamma)^s |z_0| \\
&\geq \gamma^s |\sin(u_0^k) + au_0 + c| - (1-s\gamma)|z_0| \\
&\geq \gamma^s [|\sin(u_0^k)| - |a||u_0| - |c|] - |z_0| + s\gamma|z_0| \\
&\geq s\delta [|\sin(u_0^k)| - |a||u_0| - |z_0|] - |z_0| + s\gamma|z_0| \\
&= s\delta |\sin(u_0^k)| - s\delta|a||z_0| - s\delta|z_0| - |z_0| + s\gamma|z_0| \\
&\geq s\gamma |\sin(u_0^k)| - |a||z_0| - |z_0|. \qquad (3.3)
\end{aligned}$$

We have $|\sin(u_0^k)| = |u_0^k| \left|1 - \frac{u_0^{2k}}{3!} + \frac{u_0^{4k}}{5!} - \cdots\right| \geq |u_0^k||\omega_3|$, where $|\omega_3| \in (0,1]$ except the value for which $|\omega_3| = 0$ and $|z_0| > \left(\frac{2(1+|a|)}{s\gamma|\omega_3|}\right)^{\frac{1}{k-1}}$, from inequality 3.3 we obtain

$$\begin{aligned}
|v_0| \geq & s\gamma|\omega_3||u_0^k| - (1+|a|)|z_0| \\
= & |z_0|[s\gamma|\omega_3||z_0^{k-1}| - (1+|a|)] \\
\geq & |z_0|[2(1+|a|) - (1+|a|)] \\
= & (1+|a|)|z_0| \\
\geq & |z_0|. \qquad (3.4)
\end{aligned}$$

For the next step of the four-step iteration, we have

$$\begin{aligned}
|w_0| &= |(1-\beta)^s z_0 + \beta^s T_c v_0| \\
&= |(1-\beta)^s z_0 + \beta^s(\sin(v_0^k) + av_0 + c)| \\
&\geq \beta^s |\sin(v_0^k) + av_0 + c| - (1-\beta)^s |z_0| \\
&\geq \beta^s |\sin(v_0^k) + av_0 + c| - (1-s\beta)|z_0| \\
&\geq \beta^s [|\sin(v_0^k)| - |a||v_0| - |c|] - |z_0| + s\gamma|z_0| \\
&\geq s\beta [|\sin(v_0^k)| - |a||v_0| - |z_0|] - |z_0| + s\beta|z_0| \\
&= s\beta |\sin(v_0^k)| - s\beta|a||z_0| - s\delta|z_0| - |z_0| + s\beta|z_0| \\
&\geq s\beta |\sin(v_0^k)| - |a||z_0| - |z_0|. \qquad (3.5)
\end{aligned}$$

We have $|\sin(v_0^k)| = |v_0^k| \left|1 - \frac{v_0^{2k}}{3!} + \frac{v_0^{4k}}{5!} - \cdots\right| \geq |v_0^k||\omega_2|$, where $|\omega_2| \in (0,1]$ except the

value for which $|\omega_2| = 0$ and $|z_0| > \left(\frac{2(1+|a|)}{s\beta|\omega_2|}\right)^{\frac{1}{k-1}}$, from inequality 3.5 we obtain

$$\begin{aligned}|w_0| \geq & s\beta|\omega_2||v_0^k| - (1+|a|)|z_0| \\ \geq & s\beta|\omega_2||z_0^k| - (1+|a|)|z_0| \\ = & |z_0|[s\beta|\omega_2||z_0^{k-1}| - (1+|a|)] \\ \geq & |z_0|[2(1+|a|) - (1+|a|)] \\ = & (1+|a|)|z_0| \\ \geq & |z_0|. \end{aligned} \tag{3.6}$$

For the last step of the four-step iteration, we have

$$\begin{aligned}|z_1| &= |(1-\alpha)^s z_0 + \alpha^s T_c v_0| \\ &= |(1-\beta)^s z_0 + \beta^s(\sin(w_0^k) + aw_0 + c)| \\ &\geq \alpha^s|\sin(w_0^k) + aw_0 + c| - (1-\beta)^s|z_0| \\ &\geq \beta^s|\sin(w_0^k) + aw_0 + c| - (1-s\beta)|z_0| \\ &\geq \beta^s[|\sin(w_0^k)| - |a||w_0| - |c|] - |z_0| + s\gamma|z_0| \\ &\geq s\beta[|\sin(w_0^k)| - |a||w_0| - |z_0|] - |z_0| + s\beta|z_0| \\ &= s\beta|\sin(w_0^k)| - s\beta|a||w_0| - s\delta|z_0| - |z_0| + s\beta|z_0| \\ &\geq s\beta|\sin(w_0^k)| - |a||z_0| - |z_0|. \end{aligned} \tag{3.7}$$

We have $|\sin(w_0^k)| = |w_0^k|\left|1 - \frac{w_0^{2k}}{3!} + \frac{w_0^{4k}}{5!} - \cdots\right| \geq |w_0^k||\omega_1|$, where $|\omega_1| \in (0,1]$ except the value for which $|\omega_1| = 0$ and $|z_0| > \left(\frac{2(1+|a|)}{s\alpha|\omega_1|}\right)^{\frac{1}{k-1}}$, from inequality 3.7 we obtain

$$\begin{aligned}|z_1| \geq & s\alpha|\omega_1||w_0^k| - (1+|a|)|z_0| \\ \geq & s\alpha|\omega_1||z_0^k| - (1+|a|)|z_0| \\ = & |z_0|[s\alpha|\omega_1||z_0^{k-1}| - (1+|a|)] \\ \geq & |z_0|[2(1+|a|) - (1+|a|)] \\ = & (1+|a|)|z_0|. \end{aligned} \tag{3.8}$$

From equation (3.8)

$$\begin{aligned}|z_1| \geq & (1+|a|)|z_0| \\ > & |z_0| \\ > & \max\left\{|c|, \left(\frac{2(1+|a|)}{s\alpha|\omega_1|}\right)^{\frac{1}{k-1}}, \left(\frac{2(1+|a|)}{s\beta|\omega_2|}\right)^{\frac{1}{k-1}}, \left(\frac{2(1+|a|)}{s\gamma|\omega_3|}\right)^{\frac{1}{k-1}}, \left(\frac{2(1+|a|)}{s\delta|\omega_4|}\right)^{\frac{1}{k-1}}\right\}. \end{aligned}$$

Therefore, $|z_1|$ satisfied all the conditions as $|z_0|$. So, by using the same technique for $n = 0$, we obtain the result for for $n = 1$, as

$$\begin{aligned}|z_2| \geq & (1+|a|)|z_1| \\ > & (1+|a|)^2|z_0| \end{aligned}$$

Continuing the iteration process up to the n^{th} steps, we obtain

$$|z_n| > (1+|a|)^n |z_0|.$$

Since $1+|a|>1$, we obtain $\lim_{n\to\infty} |z_n| = \infty$. □

Theorem 3.2. *Let $T_c : \mathbb{C} \to \mathbb{C}$ be a complex-valued map defined by $T_c(z) = \sin(z^k) + az + c$ for all $z \in \mathbb{C}$, $k \in \mathbb{N} \setminus \{1\}$ and $a, c \in \mathbb{C}$ such that $a \neq 0$. Consider the iterative sequence defined in (2.3) and $|\omega_1|, |\omega_2|, |\omega_3|, |\omega_4| \in (0,1]$ If*

$$|z_m| > \max\left\{|c|, \left(\frac{2(1+|a|)}{s\alpha|\omega_1|}\right)^{\frac{1}{k-1}}, \left(\frac{2(1+|a|)}{s\beta|\omega_2|}\right)^{\frac{1}{k-1}}, \left(\frac{2(1+|a|)}{s\gamma|\omega_3|}\right)^{\frac{1}{k-1}}, \left(\frac{2(1+|a|)}{s\delta|\omega_4|}\right)^{\frac{1}{k-1}}\right\}$$

for some $m \in \mathbb{N} \cup \{0\}$, then $\lim_{n\to\infty} |z_n| = \infty$.

Proof. By using a similar technique of the Theorem 3.1, we have

$$s\alpha|\omega_1||z_0|^{k-1}| - (1+|a|) > 1$$

and

$$|z_{m+n}| > |z_0|(1+|a|)^{m+n}$$

Hence, $|z_n| \to \infty$ as $n \to \infty$. □

Remark 3.3. We have

$$R = \max\left\{|c|, \left(\frac{2(1+|a|)}{s\alpha|\omega_1|}\right)^{\frac{1}{k-1}}, \left(\frac{2(1+|a|)}{s\beta|\omega_2|}\right)^{\frac{1}{k-1}}, \left(\frac{2(1+|a|)}{s\gamma|\omega_3|}\right)^{\frac{1}{k-1}}, \left(\frac{2(1+|a|)}{s\delta|\omega_4|}\right)^{\frac{1}{k-1}}\right\}$$

is called escape radius that enable the generation of novel Julia and Mandelbrot sets based on complex-valued sine functions.

4 Generation of Fractals

Fractals being produced by using Algorithm 1 (for Julia set) and Algorithm 2 (for Mandelbrot set), for creating beautiful fractal sketches for complex-valued function $T_c z = \sin(z^k) + az + c$ using a four-steps iteration process enhance with s-convexity via MATLAB R2021a on a computer system featuring an AMD Ryzen 5 7520U processor with a clock speed of 2.80 GHz, 8 GB of RAM, and running the Microsoft Windows 11 (64-bit) operating system. We employed the "Jet" colormap shown in Figure 1, a widely adopted standard colormap, to assign colors to the data points to enhance the visual representation. Our four-step iteration with given complex-valued function involves 13 parameters, it can be challenging to discuss the Julia and Mandelbrot sets comprehensively by changing all of these parameters. However, we only discuss the behavior of a fractals by varying some parameters values.

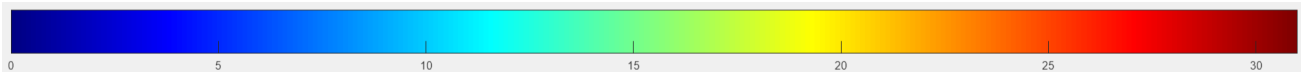

Figure 1: A colormap is used to create Julia and Mandelbrot sets.

Algorithm 1: Creating Julia set

Input: $T_c(z) = \sin(z^k) + az + c$ for all $z \in \mathbb{C}$, $k \in \mathbb{N} \setminus \{1\}$, $a, c \in \mathbb{C} : a \neq 0$ - complex constants; $B \subset \mathbb{C}$ - area; K - the maximum number of iterations; $s, \alpha, \beta, \gamma, \delta, |\omega_1|, |\omega_2|, |\omega_3|, |\omega_4| \in (0, 1]$ - parameters for the approximation of four-steps iterative method with s-convexity and colourmap $[0..F]$ - colour map with $F + 1$ colours.

Output: Julia set for area B

for $z_0 \in A$ **do**
- $R = \max\left\{|c|, \left(\frac{2(1+|a|)}{s\alpha|\omega_1|}\right)^{\frac{1}{k-1}}, \left(\frac{2(1+|a|)}{s\beta|\omega_2|}\right)^{\frac{1}{k-1}}, \left(\frac{2(1+|a|)}{s\gamma|\omega_3|}\right)^{\frac{1}{k-1}}, \left(\frac{2(1+|a|)}{s\delta|\omega_4|}\right)^{\frac{1}{k-1}}\right\}$
- $n = 0$
- $z_0 = 0$
- **while** $n \leq K$ **do**
  - $u_n = (1-\delta)^s z_n + \delta^s T_c z_n$
  - $v_n = (1-\gamma)^s z_n + \gamma^s T_c u_n$
  - $w_n = (1-\beta)^s z_n + \beta^s T_c v_n$
  - $z_{n+1} = (1-\alpha)^s z_n + \alpha^s T_c w_n$
  - **if** $|z_{n+1}| > R$ **then**
    - **break**
  - $n = n + 1$
- $i = \lfloor F\frac{n}{K} \rfloor$
- color z_0 with color map $[i]$

Algorithm 2: Creating Mandelbrot set

Input: $T_c(z) = \sin(z^k) + az + c$ for all $z \in \mathbb{C}$, $k \in \mathbb{N} \setminus \{1\}$, $a, c \in \mathbb{C} : a \neq 0$ - complex constants; $B \subset \mathbb{C}$ - area; K - the maximum number of iterations; $s, \alpha, \beta, \gamma, \delta, |\omega_1|, |\omega_2|, |\omega_3|, |\omega_4| \in (0, 1]$ - parameters for the approximation of four-steps iterative method with s-convexity; κ-critical point of T, and colourmap $[0..F]$ - colour map with $F + 1$ colours.

Output: Mandelbrot set for area B

for $c \in A$ **do**
- $R = \max\left\{|c|, \left(\frac{2(1+|a|)}{s\alpha|\omega_1|}\right)^{\frac{1}{k-1}}, \left(\frac{2(1+|a|)}{s\beta|\omega_2|}\right)^{\frac{1}{k-1}}, \left(\frac{2(1+|a|)}{s\gamma|\omega_3|}\right)^{\frac{1}{k-1}}, \left(\frac{2(1+|a|)}{s\delta|\omega_4|}\right)^{\frac{1}{k-1}}\right\}$
- $n = 0$
- $z = \kappa$
- **while** $n \leq K$ **do**
  - $u_n = (1-\delta)^s z_n + \delta^s T_c z_n$
  - $v_n = (1-\gamma)^s z_n + \gamma^s T_c u_n$
  - $w_n = (1-\beta)^s z_n + \beta^s T_c v_n$
  - $z_{n+1} = (1-\alpha)^s z_n + \alpha^s T_c w_n$
  - **if** $|z_{n+1}| > R$ **then**
    - **break**
  - $n = n + 1$
- $i = \lfloor F\frac{n}{K} \rfloor$
- color c with color map $[i]$

4.1 Julia set

In this subsection we create the Julia set by using the Algorithm 1 varying the parameters one by one. We take a maximum iteration limit of $K = 30$ and $B = [-4.5, 4.5] \times [-4.5, 4.5]$ as the area for Julia set. Initially, we fix the parameters $a = 1.2001, c = 0.501, s = 0.6767, \alpha = 0.005, \beta = 0.003, \gamma = 0.002, \delta = 0.001, \omega_1 = 0.110, \omega_2 = 0.112, \omega_3 = 0.114, \omega_4 = 0.115, k = 2$.

4.1.1 Julia set for the function $T_c z = \sin(z^k) + az + c$ varying the parameter a

Upon examining Figure 2, we observe intriguing representations of Julia sets with a degree of two while varying a parameter $a \in \mathbb{C}$. For real number a, each Julia set exhibits symmetry about the real axis. As the value of a increases, the intensity of brown color decreases, and the intensity of sky blue color increases along the axes, accompanied by a rise in the number of branches or lashes. On the other hand, when a is a complex number, each Julia set loses its symmetry, and the shape and size remain almost constant for all complex numbers of a, which we are taking for investigation.

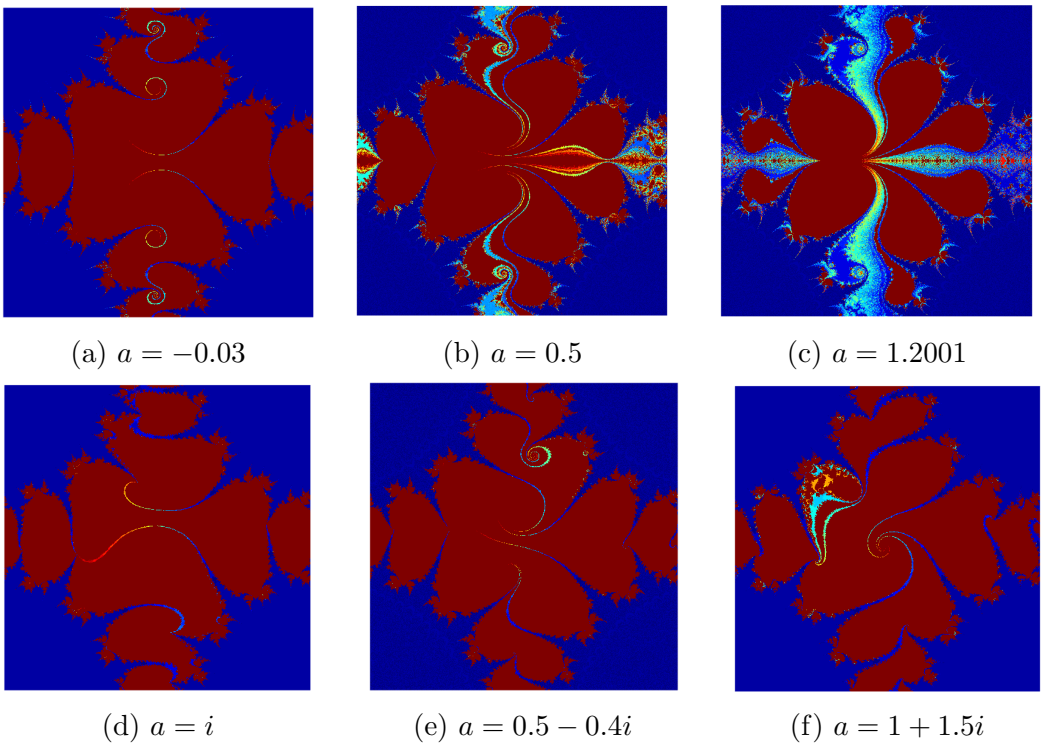

(a) $a = -0.03$ (b) $a = 0.5$ (c) $a = 1.2001$

(d) $a = i$ (e) $a = 0.5 - 0.4i$ (f) $a = 1 + 1.5i$

Figure 2: The impact on Julia sets for varying the parameter a

4.1.2 Julia set for the function $T_c z = \sin(z^k) + az + c$ varying the parameter c

We observe captivating depictions of Julia sets with a degree of two, varying a parameter a as illustrated in Figure 3. When a is a real number, each Julia set displays symmetry about the real axis. With an increase in the value of a, there is an augmentation in the intensity of brown color, accompanied by a decrease in the intensity of sky blue. Simultaneously, there is a reduction in the number of branches or lashes, and the size of the set increases. Conversely, when a is a complex number, each Julia set loses its symmetry, and lashes are formed more arbitrarily. The mesmerizing Julia sets mainly manifest when the parameter a is a real number.

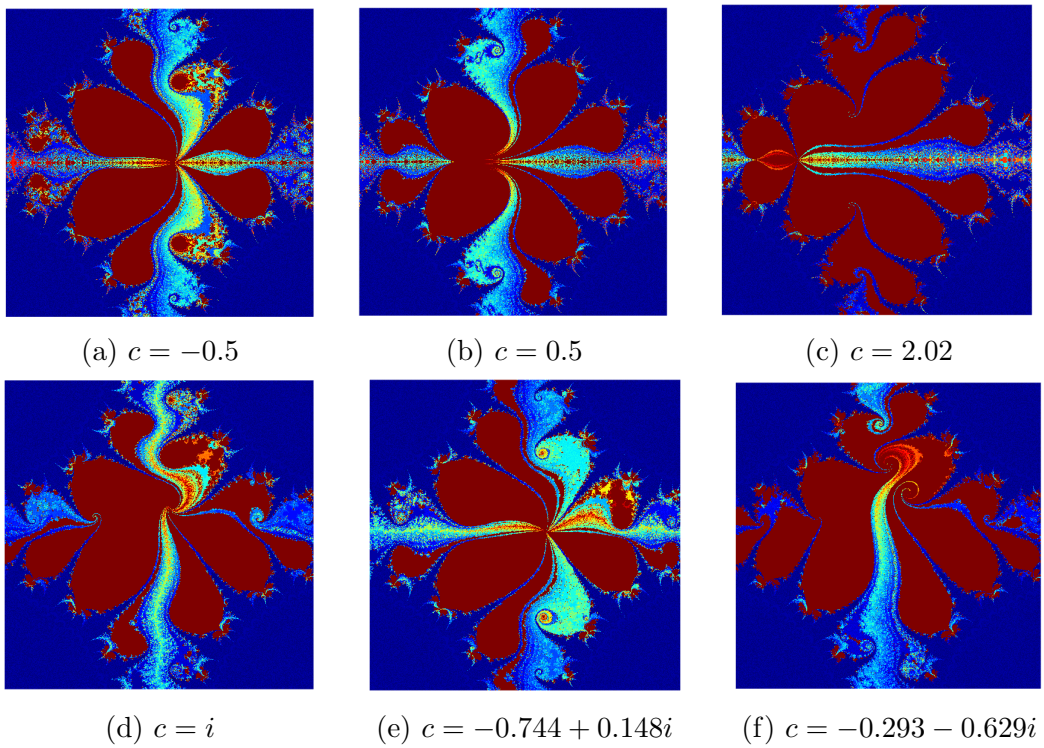

(a) $c = -0.5$ (b) $c = 0.5$ (c) $c = 2.02$

(d) $c = i$ (e) $c = -0.744 + 0.148i$ (f) $c = -0.293 - 0.629i$

Figure 3: The impact on Julia sets for varying the parameter c

4.1.3 Julia set for the function $T_c z = \sin(z^k) + az + c$ varying the convexity parameter s

We observe stunning representations of Julia sets with a degree of two, varying a parameter s as shown in Figure 4. When the value of s is small, approaching zero, most points in the considered area escape to infinity, resulting in a minor, undeclared Julia set with a predominant sky blue color. As s increases, the size of the Julia set also increases, accompanied by an intensification of the brown and yellow color and a reduction in the intensity of the sky-blue hue. Additionally, the boundary exhibits numerous lashes. When s approaches 1, the Julia set is predominantly filled with brown color. Interestingly, for all the values of s considered in our observations, each Julia set maintains symmetry with respect to the real axis.

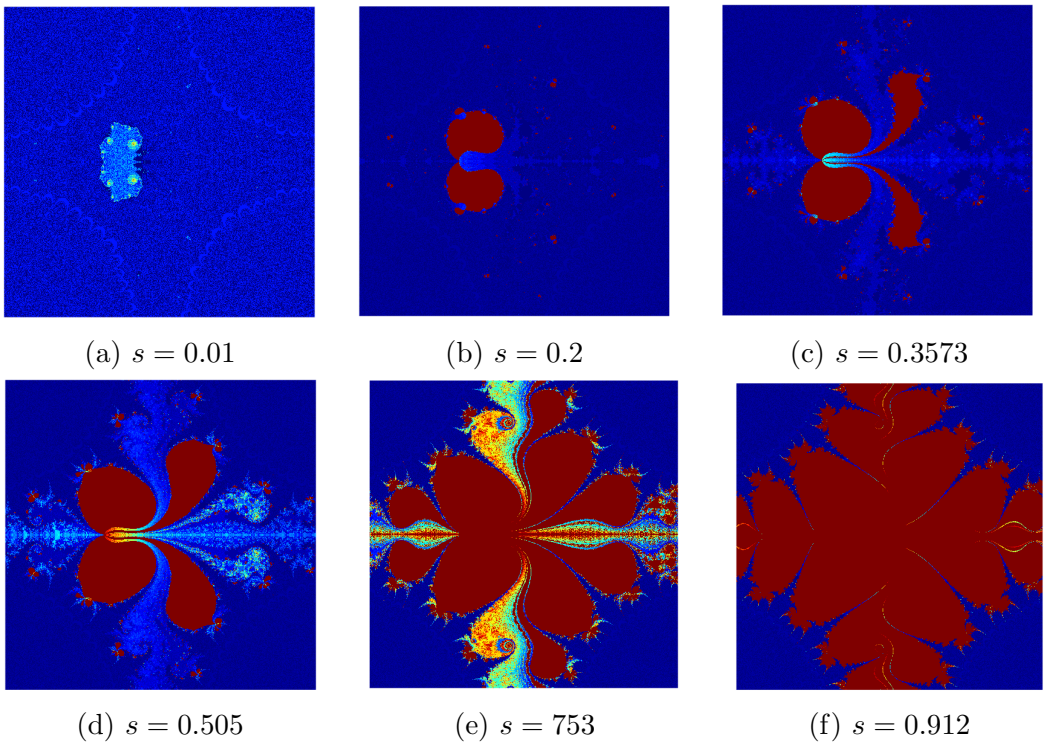

(a) $s = 0.01$ (b) $s = 0.2$ (c) $s = 0.3573$

(d) $s = 0.505$ (e) $s = 753$ (f) $s = 0.912$

Figure 4: The impact on Julia sets for varying the convexity parameter s

4.1.4 Julia set for the function $T_c z = \sin(z^k) + az + c$ varying the parameter α

We observe captivating depictions of Julia sets with a degree of two while varying a parameter α as illustrated in Figure 5. When the value of α is close to zero, indicating a minimal value, the intensity of the brown color is high. Each lash is fully developed, featuring tiny lashes at the tip, and lashes look like cactus leaves. In this scenario, there are more non-escaping points within the considered area. As α increases, the number of escaping points also increases, resulting in a decrease in the size of Julia sets. Simultaneously, the intensity of brown color decreases, and the intensity of the sky blue hue increases. For values of α approaching 1, the brown color is completely removed, causing the Julia set to appear weakened, making the details less clearly visible. Notably, for each value of α, the Julia sets exhibit symmetry about the real axis.

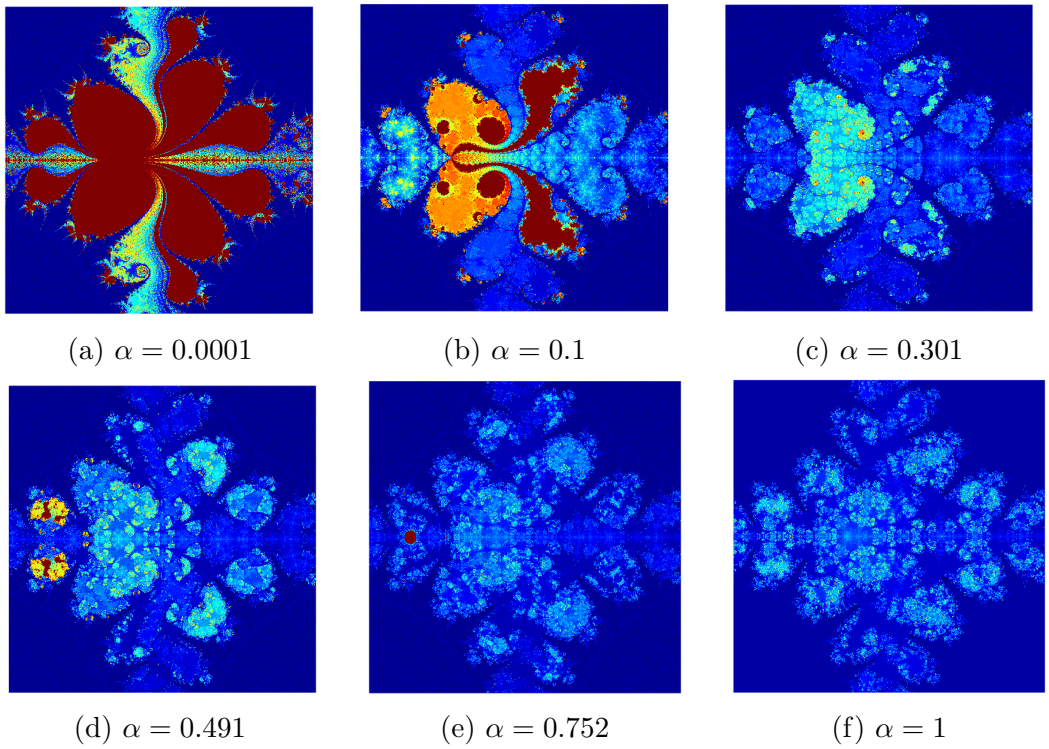

(a) $\alpha = 0.0001$ (b) $\alpha = 0.1$ (c) $\alpha = 0.301$

(d) $\alpha = 0.491$ (e) $\alpha = 0.752$ (f) $\alpha = 1$

Figure 5: The impact on Julia sets for varying the parameter α

4.1.5 Julia set for the function $T_c z = \sin(z^k) + az + c$ varying the parameter β

We observe captivating depictions of Julia sets with a degree of two, varying a parameter β as shown in Figure 6. For each value of β, the Julia sets maintain symmetry about the real axis. When the value of β approaches zero, the brown color intensity is high, and each lash is fully developed with tiny lashes at the tip, resembling cactus leaves and forming intricate Julia sets. In this scenario, there are more non-escaping points within the considered area. With increasing values of β, the number of escaping points also rises, reducing the size of Julia sets. Concurrently, the intensity of the brown color diminishes ultimately after $\beta \geq 0.312$, leaving only the sky blue hue. This causes the Julia set to appear weakened, resulting in less clear visibility of details.

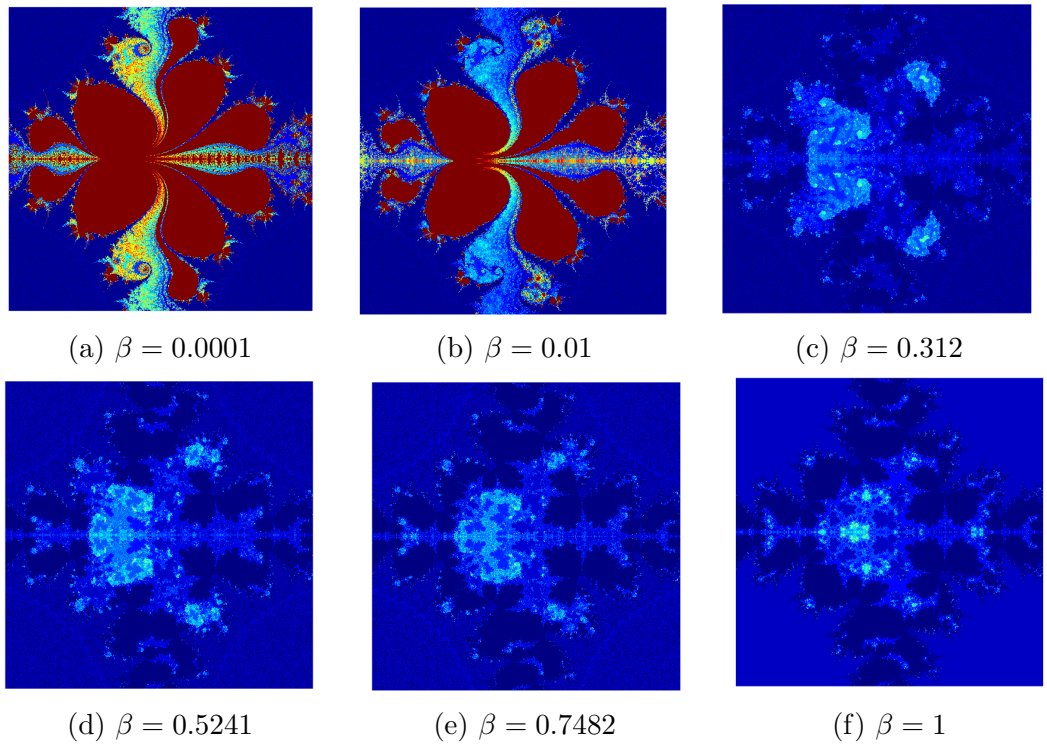

(a) $\beta = 0.0001$ (b) $\beta = 0.01$ (c) $\beta = 0.312$

(d) $\beta = 0.5241$ (e) $\beta = 0.7482$ (f) $\beta = 1$

Figure 6: The impact on Julia sets for varying the parameter β

4.1.6 Julia set for the function $T_c z = \sin(z^k) + az + c$ varying the parameter β

We observe fascinating depictions of Julia sets with a degree of two, varying a parameter β as shown in Figure 7. For each value of β, the Julia sets maintain symmetry about the real axis. When the value of β approaches zero, the brown color intensity is high, and each lash is fully formed with tiny lashes at the end, resembling cactus leaves and intricate Julia sets. In this procedure, there are more non-escaping points within the considered area. With increasing values of β, the number of escaping points also rises, reducing the size of Julia sets. Concurrently, the intensity of the brown color diminishes ultimately after $\beta \geq 0.312$; only the sky blue hue is present, and the Julia set appears weakened, resulting in less clear visibility of details.

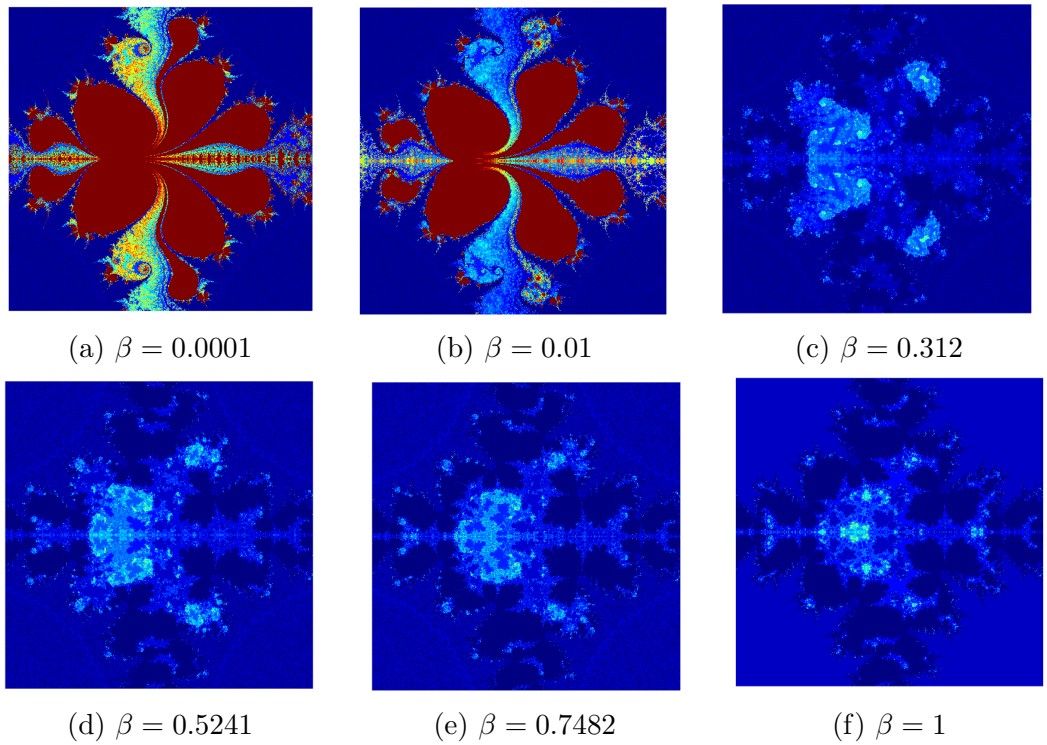

(a) $\beta = 0.0001$ (b) $\beta = 0.01$ (c) $\beta = 0.312$

(d) $\beta = 0.5241$ (e) $\beta = 0.7482$ (f) $\beta = 1$

Figure 7: The impact on Julia sets for varying the parameter β

4.1.7 Julia set for the function $T_c z = \sin(z^k) + az + c$ varying the parameter γ

We observe captivating depictions of Julia sets with a degree of two while manipulating a parameter γ as depicted in Figure 8. Notably, for each value of γ, the Julia sets exhibit symmetry with respect to the real axis.

When γ is close to zero, a striking Julia set is formed with a high-intensity brown color. Numerous lashes are present, each exhibiting a shape reminiscent of cactus leaves. This configuration results in a visually appealing Julia set with intricate details. As the value of γ increases, there is a reduction in the size of Julia sets, accompanied by a decrease in the number of lashes and a diminishing intensity of brown color.

After γ exceeds 0.2, the brown color completely disappears, and only the sky blue color remains in the Julia sets. These sets require more prominence, making perceiving the finer details difficult. This transition suggests that as γ approaches one, the number of escaping points increases, significantly altering the Julia sets' visual characteristics.

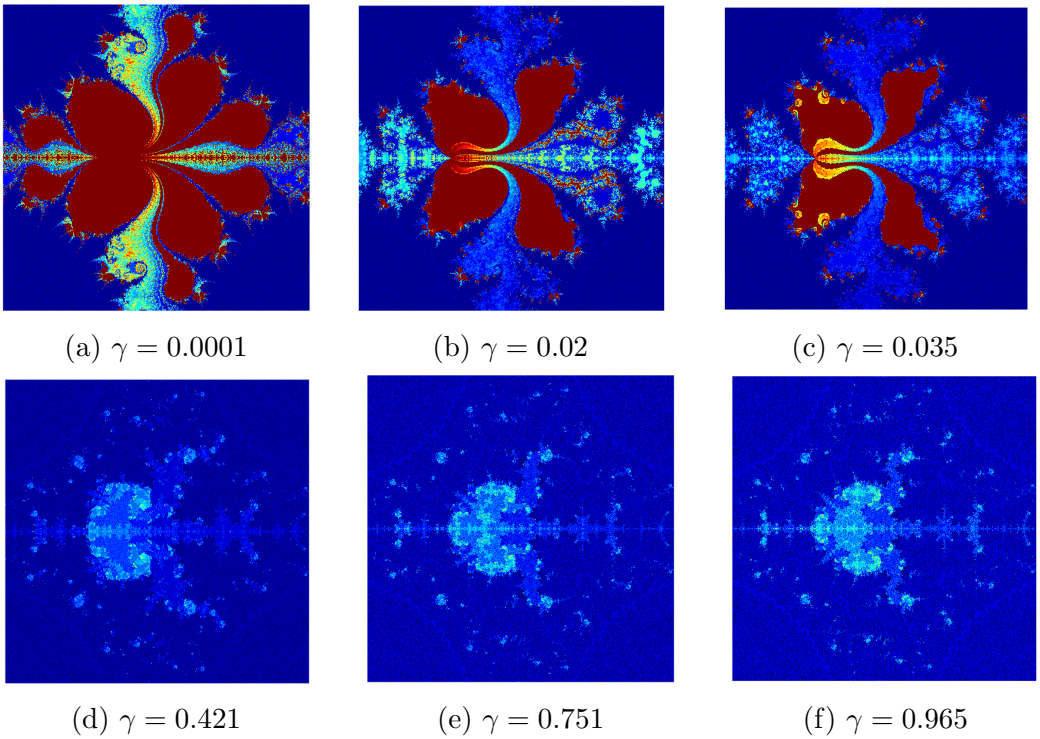

(a) $\gamma = 0.0001$ (b) $\gamma = 0.02$ (c) $\gamma = 0.035$

(d) $\gamma = 0.421$ (e) $\gamma = 0.751$ (f) $\gamma = 0.965$

Figure 8: The impact on Julia sets for varying the parameter γ

4.1.8 Julia set for the function $T_c z = \sin(z^k) + az + c$ varying the parameter δ

We observe enchanting illustrations of quadratic Julia sets while altering a parameter δ as illustrated in Figure 9. Notably, for each value of δ, the Julia sets preserve symmetry regarding the real axis.

When δ approaches zero, an impressive Julia set emerges, characterized by a rich, high-intensity brown color. The set features numerous lashes, each resembling the shape of cactus leaves, resulting in a visually appealing and intricately detailed Julia set. Many tiny lashes are present at the tip of each central lash. As the value of δ increases, there is a noticeable reduction in the size of the Julia sets, accompanied by a decrease in the number and size of lashes and a gradual reduction in the intensity of the brown color.

When $\delta > 0.1$, the brown color completely vanishes, leaving Julia's sets dominated by a sky blue color behind. However, these sets require heightened prominence, and discerning finer details becomes challenging. This shift implies that as δ approaches one, the number of points escaping to infinity increases, leading to a significant transformation in the visual characteristics of the Julia sets.

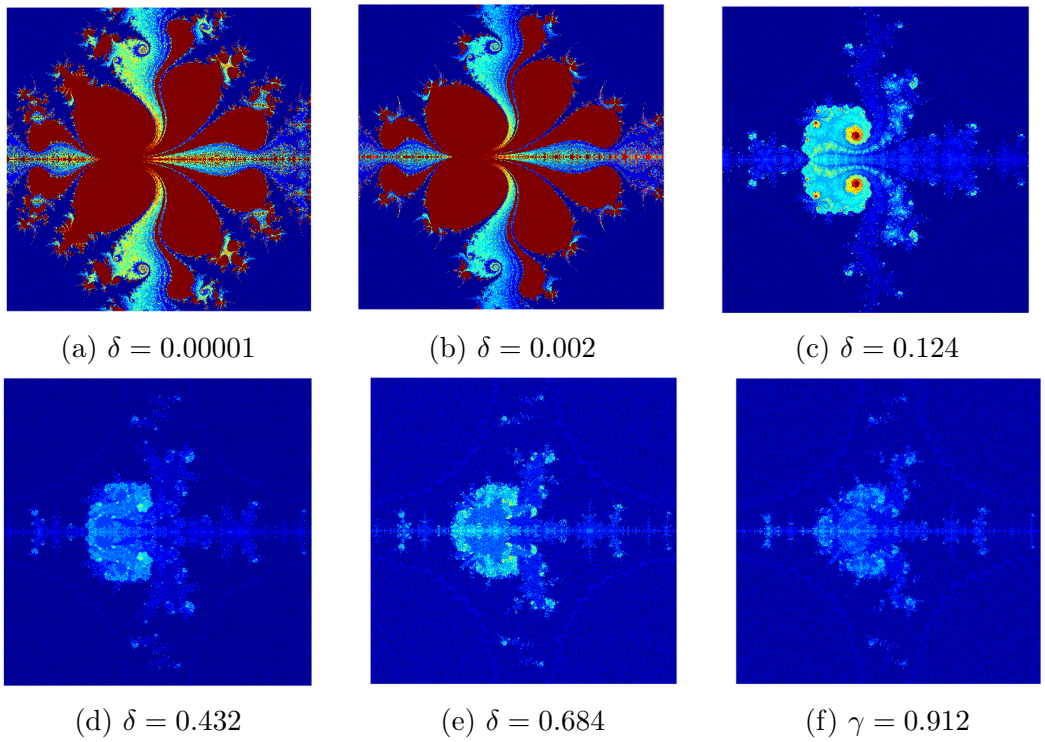

(a) $\delta = 0.00001$ (b) $\delta = 0.002$ (c) $\delta = 0.124$

(d) $\delta = 0.432$ (e) $\delta = 0.684$ (f) $\gamma = 0.912$

Figure 9: The impact on Julia sets for varying the parameter δ

4.1.9 Julia set for the function $T_c z = \sin(z^k) + az + c$ varying the k

We generate captivating fractal patterns, as illustrated in Figure 10, by varying the parameter k. For $k = 2$, the resulting Julia set displays four distinct lashes formed by blending sky blue, light yellow, and brown colors along the real and imaginary axes. Additionally, numerous cactus leaf-like lashes with a brown hue are present within the Julia set. When $k = 3$, the outer part of the Julia set exhibits six lashes with a sky blue color, while the inner region features numerous lashes with a brown hue. As the value of the parameter k increases, the size of the Julia set decreases, and the set adopts a more circular shape. Each Julia set, regardless of the value of k, showcases $2k$ outer lashes, with smaller lashes forming in the central region. The Julia set is more aesthetically pleasing when the parameter k is lower.

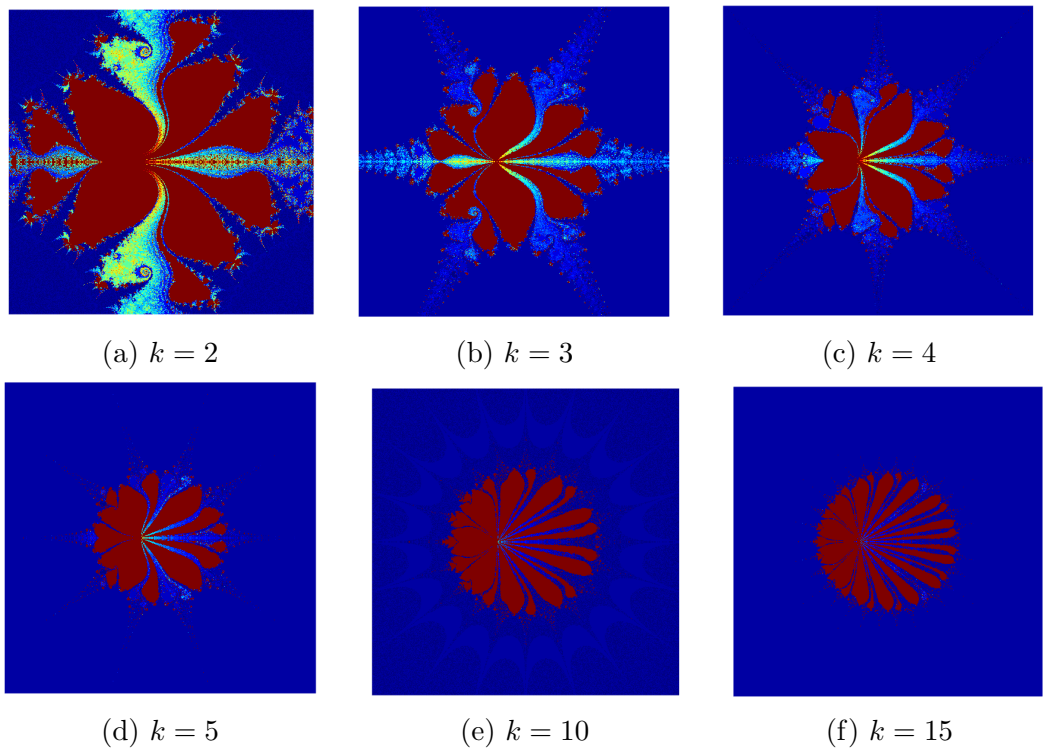

(a) $k = 2$ (b) $k = 3$ (c) $k = 4$

(d) $k = 5$ (e) $k = 10$ (f) $k = 15$

Figure 10: The impact on Julia sets for varying k

4.2 Mandelbrot set

In this segment, we generate Mandelbrot sets using Algorithm 2. We systematically vary each parameter individually while keeping the remaining parameters fixed, discussing the resulting properties. We set the maximum iteration limit to $K = 30$, and define the area for the Mandelbrot set as $B = [-3.5, 3.5] \times [-3.5, 3.5]$. Initially, we set the parameters to specific values: $a = -0.51, s = 0.5001, \alpha = 0.0078, \beta = 0.0056, \gamma = 0.0046, \delta = 0.00, \omega_1 = 0.8383, \omega_2 = 0.119, \omega_3 = 0.7474, \omega_4 = 0.6556$, and $k = 2$.

4.2.1 Mandelbrot set for the function $T_c z = \sin(z^k) + az + c$ varying the parameter a

We generate captivating fractal patterns, as depicted in Figure 11, by manipulating the parameter a. When a is a real number, specifically $a = -0.51$, a prominent cardioid shape dominates the center of the Mandelbrot set. The size of this cardioid diminishes continuously along the real axis, creating a sequence of progressively smaller cardioids. As a increases, the size of the Mandelbrot set decreases, accompanied by a reduction in the intensity of the brown color. This decrease in intensity signifies that an increasing number of points within the considered area escape to infinity as a increases. Each Mandelbrot set, corresponding to a real number a, maintains symmetry about the real axis.

On the other hand, when a is a complex number, the symmetry of the Mandelbrot sets becomes less pronounced, introducing twists in the patterns. The resulting images display a more chaotic arrangement, making interpreting the details difficult.

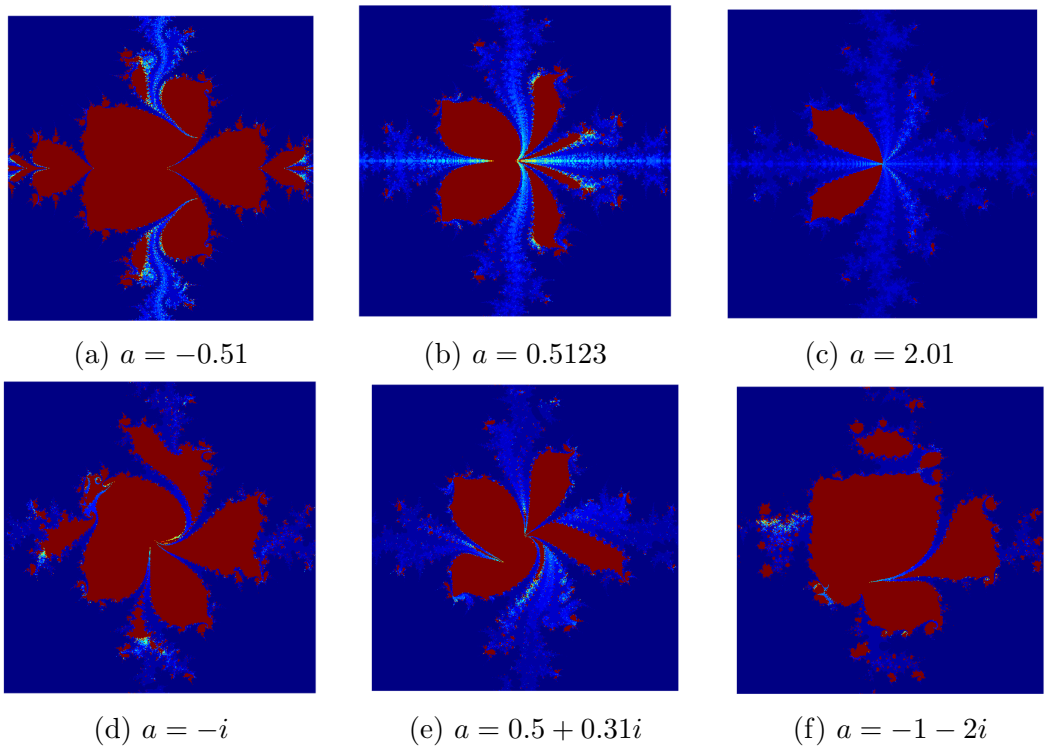

(a) $a = -0.51$ (b) $a = 0.5123$ (c) $a = 2.01$

(d) $a = -i$ (e) $a = 0.5 + 0.31i$ (f) $a = -1 - 2i$

Figure 11: The impact on Julia sets for varying a

4.2.2 Mandelbrot set for the function $T_c z = \sin(z^k) + az + c$ varying the parameter s

We create mesmerizing fractal patterns, as showcased in Figure 12, by varying the parameter s. For each value of s yields, Mandelbrot sets that exhibit a symmetrical about the real axis. In instances where s is close to zero, signifying a small value, the resulting Mandelbrot sets are characterized by reduced size, indicating most points within the defined area escape to infinity. As we increment the value of s, the size of the Mandelbrot sets gradually enlarges. Simultaneously, there is a discernible augmentation in the intensity of the brown color, creating a visually dynamic effect. Eventually, when s approaches a value close to 1, the entire Mandelbrot set adopts a uniform brown hue, providing a fascinating visual outcome.

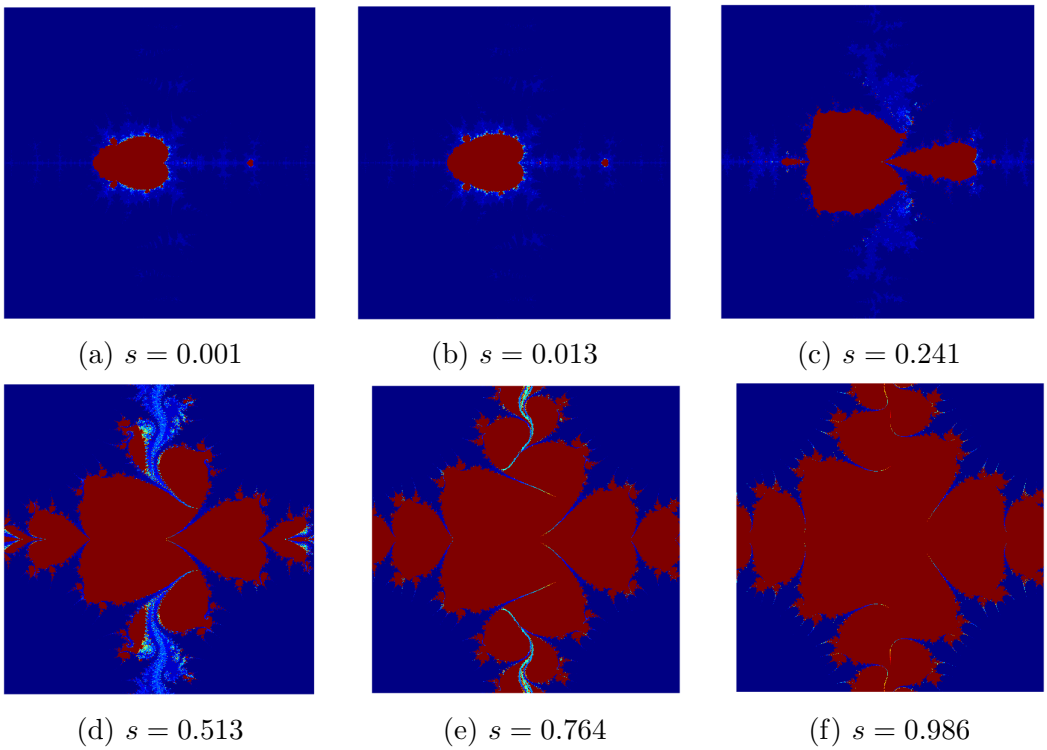

(a) $s = 0.001$ (b) $s = 0.013$ (c) $s = 0.241$

(d) $s = 0.513$ (e) $s = 0.764$ (f) $s = 0.986$

Figure 12: The impact on Mandelbrot sets for varying the parameter s

4.2.3 Mandelbrot set for the function $T_c z = \sin(z^k) + az + c$ varying the parameter α

We generate captivating fractal patterns, as depicted in Figure 13, by adjusting the parameter α. Each specific value of α produces Mandelbrot sets with symmetrical arrangements about the real axis. Notably, when α is close to zero, signifying a small value, the resulting Mandelbrot sets are characterized by a significant size, showcasing a remarkable structure reminiscent of beautiful, hair-like patterns. The entire set is adorned with a rich brown color, creating an aesthetically pleasing and intricate design.

As α increases, a notable transformation occurs. The size of the Mandelbrot sets gradually diminishes, accompanied by an increase in the intensity of the sky-blue hue along the boundary of the sets. This alteration in color dynamics adds a captivating contrast to the fractal patterns. When α approaches a value near 1, a distinct visual effect emerges. The Mandelbrot set becomes disconnected and elongated along the real axis, presenting a unique and intriguing characteristic that sets it apart from the patterns observed at lower α values. This variation in structure and coloration showcases the sensitivity of the fractal patterns to changes in the parameter α.

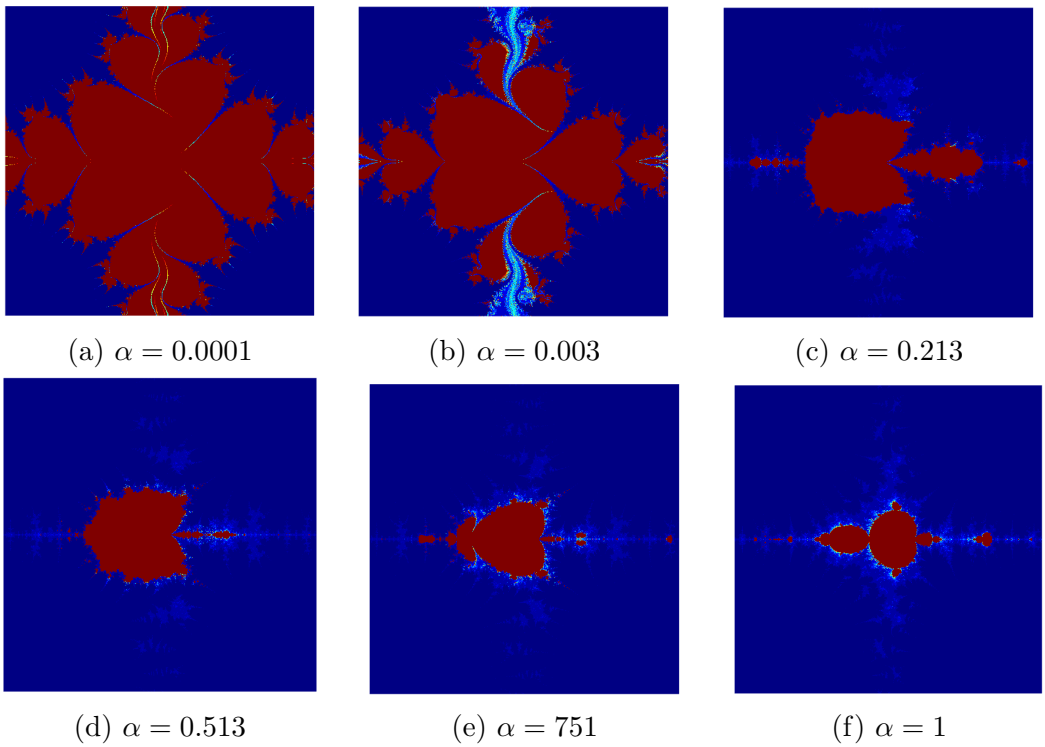

(a) $\alpha = 0.0001$ (b) $\alpha = 0.003$ (c) $\alpha = 0.213$

(d) $\alpha = 0.513$ (e) $\alpha = 751$ (f) $\alpha = 1$

Figure 13: The impact on Mandelbrot sets for varying the parameter α

4.2.4 Mandelbrot set for the function $T_c z = \sin(z^k) + az + c$ varying the parameter β

We generate captivating fractal patterns, as illustrated in Figure 14, by manipulating the parameter β. Each specific value of β results in Mandelbrot sets exhibiting symmetrical arrangements about the real axis. When β is close to zero, the resulting Mandelbrot sets showcase a substantial size, featuring two prominent sky-blue lashes along the imaginary axis. The entirety of the set is adorned with a rich brown color, contributing to an aesthetically pleasing and intricate design.

As β increases, a significant transformation unfolds. The size of the Mandelbrot sets gradually diminishes, concurrent with an intensification of the sky-blue hue along the sets' boundaries. This shift in color dynamics introduces a captivating contrast to the fractal patterns. A distinct visual effect emerges as β approaches a value near 1. The Mandelbrot set takes on a disconnected and elongated form along the real axis, and small dot-like structures in yellow color become apparent on the outer parts of the Mandelbrot sets. This variation in structure and coloration underscores the sensitivity of the fractal patterns to alterations in the parameter β.

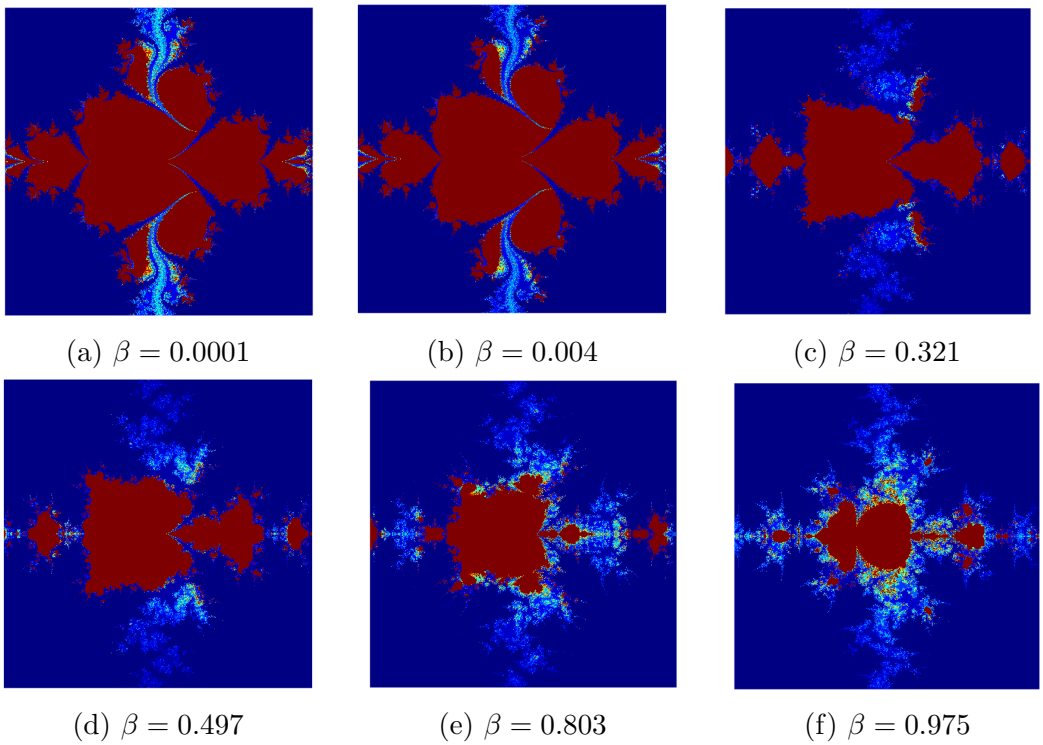

(a) $\beta = 0.0001$ (b) $\beta = 0.004$ (c) $\beta = 0.321$

(d) $\beta = 0.497$ (e) $\beta = 0.803$ (f) $\beta = 0.975$

Figure 14: The impact on Mandelbrot sets for varying the parameter β

4.2.5 Mandelbrot set for the function $T_c z = \sin(z^k) + az + c$ varying the parameter γ

We create captivating fractal patterns, as depicted in Figure 15, by varying the parameter γ. Each specific value of γ gives rise to Mandelbrot sets that exhibit symmetrical arrangements about the real axis. When γ is close to zero, the resulting Mandelbrot sets display a significant size, featuring two prominent sky-blue lashes along the imaginary axis. The entire set is adorned with a rich brown color, contributing to an aesthetically pleasing and intricate design. This configuration showcases the sensitivity of the fractal patterns to variations in the parameter γ, producing visually dynamic and appealing results. With an increase in γ, the size of the Mandelbrot sets gradually decreases, accompanied by an intensification of the sky-blue hue along the boundaries of the sets. This alteration in color dynamics introduces a captivating contrast to the fractal patterns. A distinct visual effect emerges as γ approaches a value near 1, and small dot-like structures in yellow color become apparent on the outer parts of the Mandelbrot sets. This variation in structure and coloration highlights the sensitivity of the fractal patterns to changes in the parameter γ, resulting in visually dynamic and intriguing patterns.

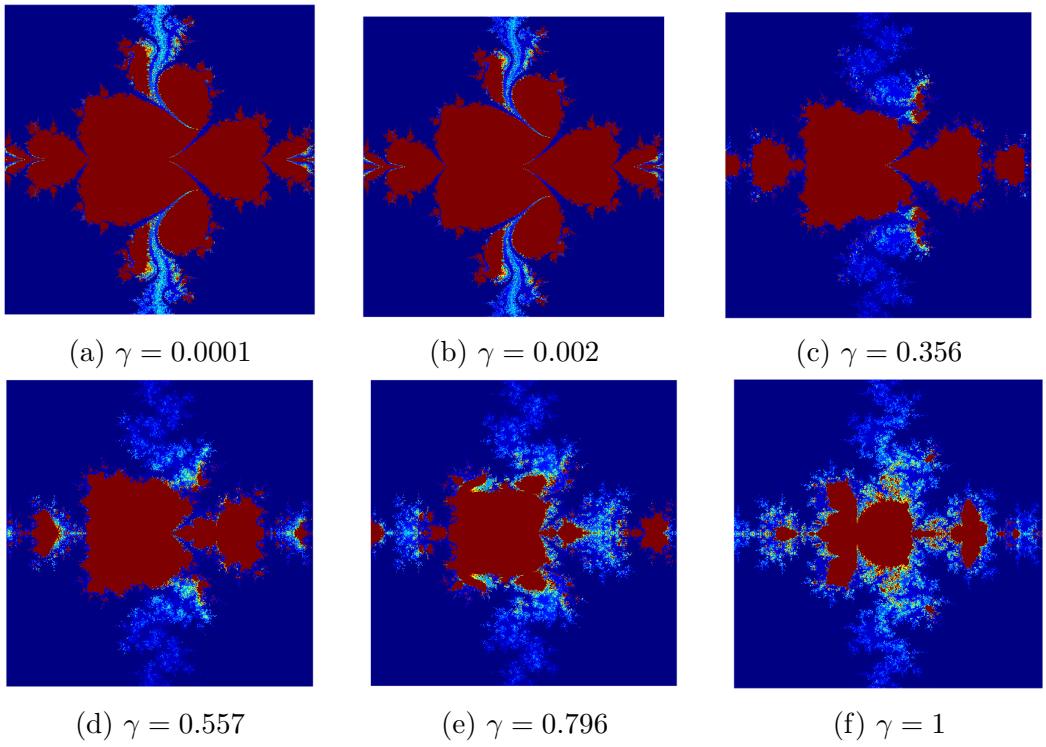

(a) $\gamma = 0.0001$ (b) $\gamma = 0.002$ (c) $\gamma = 0.356$

(d) $\gamma = 0.557$ (e) $\gamma = 0.796$ (f) $\gamma = 1$

Figure 15: The impact on Mandelbrot sets for varying the parameter γ

4.2.6 Mandelbrot set for the function $T_c z = \sin(z^k) + az + c$ varying the parameter δ

We generate captivating fractal patterns, as illustrated in Figure 16, by varying the parameter δ. Each δ results in Mandelbrot sets that exhibit symmetrical arrangements about the real axis. When δ is close to zero, the resulting Mandelbrot sets showcase a significant size, featuring two prominent sky-blue lashes along the imaginary axis. The entire set is adorned with a rich brown color, contributing to an aesthetically pleasing and intricate design.

As δ increases, the size of the Mandelbrot sets gradually diminishes, accompanied by an intensification of the sky-blue hue along the boundaries of the sets. A distinct visual effect emerges as δ approaches a value near 1, and small dot-like structures in yellow color become apparent on the outer parts of the Mandelbrot sets. This variation in structure and coloration highlights the sensitivity of the fractal patterns to changes in the parameter δ, resulting in visually dynamic and intriguing patterns.

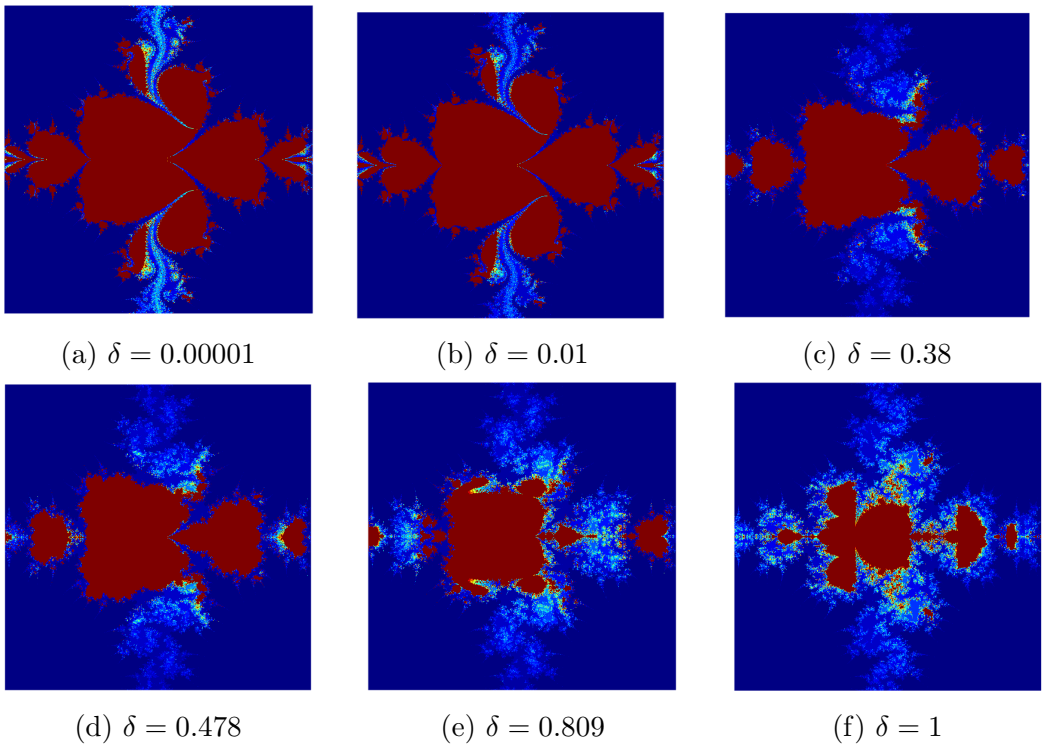

(a) $\delta = 0.00001$ (b) $\delta = 0.01$ (c) $\delta = 0.38$

(d) $\delta = 0.478$ (e) $\delta = 0.809$ (f) $\delta = 1$

Figure 16: The impact on Mandelbrot sets for varying the parameter δ

4.2.7 Mandelbrot set for the function $T_c z = \sin(z^k) + az + c$ varying the parameter k

We generate captivating fractal patterns, as showcased in Figure 17, by varying the parameter k. The behavior of the Mandelbrot sets is contingent on whether k is an even or odd natural number. For even values of k, the resulting fractals display symmetry solely concerning the real axis. In contrast, when k is an odd natural number, the Mandelbrot sets exhibit symmetrical characteristics about both the real and imaginary axes.

For the specific case of $k = 3$, the fractals have a unique appearance reminiscent of a brown spider-like shape. As the parameter k increases, there is a noticeable reduction in the size of the Mandelbrot sets. The sets transform into circular shapes, and the number of primary lashes corresponds to $k - 1$. Additionally, intricate structures emerge at the tips of each lash, adding complexity to the overall visual composition. This detailed variation in the value of k significantly influences the Mandelbrot sets' symmetry, size, and the formation of intricate details in the fractal patterns.

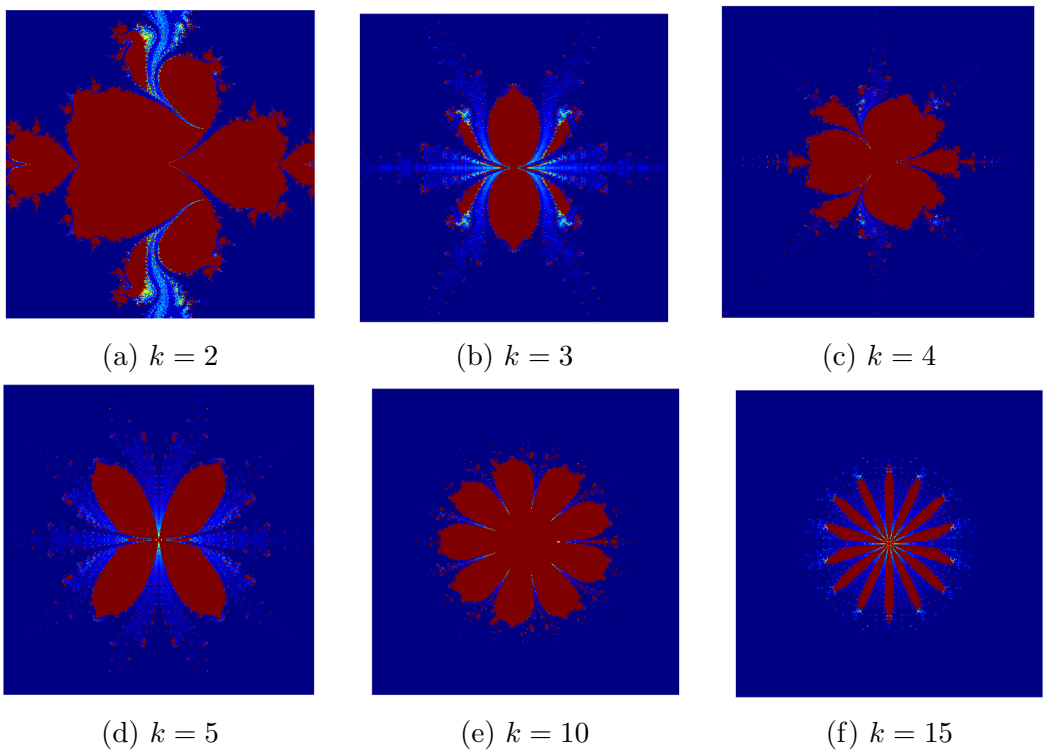

(a) $k = 2$ (b) $k = 3$ (c) $k = 4$

(d) $k = 5$ (e) $k = 10$ (f) $k = 15$

Figure 17: The impact on Mandelbrot sets for varying the parameter k

5 Conclusions

Certainly! The paper discusses a novel approach for establishing escape criteria for the complex sine function $T_c(z) = \sin(z^k) + az + c$. The method involves a four-step iterative scheme extended with s-convexity. This approach is implemented in Algorithms 1 and 2, which enable the visualization of Julia and Mandelbrot sets through a four-step iteration orbit.

The size of the generated fractals is influenced by the convexity parameter s, with larger values of s generally resulting in larger fractals. However, when parameters like α, β, γ, and δ approach 1, the size of the fractals decreases, and many points escape to infinity, making the images of the fractals weaker.

Parameters a and c play a crucial role in determining the specific shape and symmetry of the fractals. Changing these parameters leads to different patterns, symmetries, and visual characteristics in the generated fractals. Notably, certain fractals exhibit patterns resembling spiders, flowers, or other natural phenomena, emphasizing the fascinating connection between mathematical fractals and the complexity found in nature.

The parameter k is discussed as influencing the compactness and appearance of the fractals. Higher values of k result in more compact fractals with circular or rounded shapes, featuring numerous lashes in the case of Julia sets and $k - 1$ lashes in the case of Mandelbrot sets. This change in shape is attributed to the iterative process and the

specific dynamics of the underlying function.

The paper suggests practical applications in the cloth and ceramics industries. Textile engineers can utilize the generated fractal patterns to design unique and visually appealing fabric patterns. The findings of the paper contribute to a deeper understanding of the behavior and characteristics of fractal sets, showcasing the potential of the four-step iteration scheme in generating intricate and captivating fractals.

The future direction mentioned involves extending the results for the Jungck-four step iteration with s-convexity, indicating potential advancements and applications of the proposed methodology.

Acknowledgement

Acknowledging the referee's contribution to enhancing the readability of this paper is essential. Their valuable feedback and suggestions likely played a crucial role in refining the clarity and coherence of the content, ensuring that the research findings were effectively communicated to the intended audience.

References

[1] M. Abbas, H. Iqbal, and M. De la Sen. Generation of Julia and Madelbrot Sets via Fixed Points. *Symmetry*, 12:1–19, 01 2020.

[2] N. Adhikari and W. Sintunavarat. Exploring the Julia and Mandelbrot Sets of $z^p + \log c^t$ Using a Four-step Iteration Scheme Extended with s-Convexity. *Mathematics and Computers in Simulation*, 220:357–381, 2024.

[3] N. Adhikari and W. Sintunavarat. The Julia and Mandelbrot Sets for the Complex-Valued Function Exhibit Mann and Picard–Mann Orbits Along with s-Convexity. *Chaos, Solitons and Fractals*, 181:114600, 2024.

[4] D. Ashish, M. Rani, and R. Chugh. Julia Sets and Mandelbrot Sets in Noor Orbit. *Applied Mathematics and Computation*, 228:615–631, 02 2014.

[5] P. Fatou. Sur les Substitutions Rationnelles. *C. R. Acad. Sci. Paris*, 164:806–808, 1917.

[6] G. Julia. Mémoire Sur L'itération Des Fonctions Rationnelles. *J. Math. Pures Appl.*, 8:47–74, 1918.

[7] M. Kumari, D. Ashish, and R. Chugh. New Julia and Mandelbrot Sets for a New Faster Iterative Process. *International Journal of Pure and Apllied Mathematics*, 107:161–177, 03 2016.

[8] S. Kumari, K. Gdawiec, A. Nandal, M. Postolache, and R. Chugh. A Novel Approach to Generate Mandelbrot Sets, Julia Sets and Biomorphs via Viscosity Approximation Method. *Chaos, Solitons and Fractals*, 163:1–21, 10 2022.

[9] A. Lakhtakia, V. V. Varadan, R. Messier, and Varadan. On the Symmetries of the Julia Sets for the Process $z^p + c$. *Journal of Physics A: Mathematical and Theoretical*, 20(11):3533 –3535, 12 1987.

[10] X. Liu, Z. Zhu, G. Wang, and W. Zhu. Composed Accelerated Escape Time Algorithm to Construct the General Mandelbrot Sets. *Fractals*, 09:1–20, 11 2011.

[11] B. Mandelbrot. *The Fractal Geometry of Nature*. W. H. Freeman: New York, 1982.

[12] M. Pinheiro. S-convexity Foundations for Analysis. *Differential Geometry–Dynamical Systems*, pages 257–262, 2008.

[13] B. Prasad and K. Katiyar. Fractals via Ishikawa Iteration. *Communications in Computer and Information Science*, 140:197–203, 01 2011.

[14] M. Rani and R. Agarwal. Effect of Stochastic Noise on Superior Julia Sets. *J. Math. Imaging Vis.*, 36:63–68, 2010.

[15] A. Shahid, W. Nazeer, and K. Gdawiec. The Picard–Mann Iteration with s-convexity in the Generation of Mandelbrot and Julia Sets. *Monatshefte für Mathematik*, 195:1–20, 08 2021.

[16] W. Shatanawi, A. Bataihah, and A. Tallafha. Four-Step Iteration Scheme to Approximate Fixed Point for Weak Contractions. *Computers, Materials & Continua*, 64:1491–1504, 06 2020.

[17] M. Tanveer, W. Nazeer, and K. Gdawiec. New Escape Criteria for Complex Fractals Generation in Jungck-CR Orbit. *Indian Journal of Pure and Applied Mathematics*, 51:1285–1303, 12 2020.

[18] A. Tassaddiq. General Escape Criteria for the Generation of Fractals in Extended Jungck–Noor Orbit. *Mathematics and Computers in Simulation*, 196:1–14, 2022.

[19] A. Tomar, S. Antal, D. Prajapati, and P. Agarwal. Mandelbrot Fractals using Fixed-Point Technique of Sine Function. *Proceedings of the Institute of Mathematics and Mechanics National Academy of Sciences of Azerbaijan*, 48:194–214, 11 2022.

[20] A. Tomar, V. Kumar, U. Rana, and M. Sajid. Fractals as Julia and Mandelbrot Sets of Complex Cosine Functions via Fixed Point Iterations. *Symmetry*, 2023:1–21, 02 2023.

[21] C. Zou, A. Shahid, A. Tassaddiq, A. Khan, and M. Ahmad. Mandelbrot Sets and Julia Sets in Picard-Mann Orbit. *IEEE Access*, 8:64411–64421, 03 2020.